# Sheffield Hallam University

# A comparison of microstructure and mechanical properties of low-alloy-medium-carbon steels after quench-hardening

ABBASI, Erfan <http://orcid.org/0000-0001-6252-5425>, LUO, Quanshun <http://orcid.org/0000-0003-4102-2129> and OWENS, Dave

**Citation:**

**Highlights**

1. Martensite refinement was mainly associated with chemical composition of steel.

2. A larger volume fraction of retained austenite in NiCrSi and NiCrMoV steels was mainly attributed to their chemical composition.

3. A higher strength of NiCrSi and NiCrMoV steels was ascribed to their finer prior austenite grain size, higher dislocation density and chemical composition, particularly higher carbon content.

4. The degree of interface decohesion between the martensite matrix and inclusions increased as the strength of martensite increased.

# A Comparison of Microstructure and Mechanical Properties of Low-Alloy-Medium-Carbon Steels after Quench-hardening

Erfan Abbasi [a,b,*], Quanshun Luo [a], Dave Owens [b]

[a] Materials and Engineering Research Institute, Sheffield Hallam University, Howard Street, Sheffield, S1 1WB, UK; [b] Tyzack Machine Knives Ltd, Shepcote Lane, Sheffield, S9 1TG, UK

* Corresponding author. Tel.: +44 (0) 114 221 1059, E-mail address: engabasi@gmail.com (E. Abbasi)

## Abstract

The microstructural characteristics of three medium carbon steels, namely MnCrB, NiCrSi and NiCrMoV containing steels, have been investigated when the steels were hardened by quenching in water or oil from different austenitisation temperatures (i.e. 850, 900 and 950 °C). The microstructure was characterised using optical microscopy, scanning electron microscopy and energy dispersive X-ray spectroscopy, and X-Ray diffraction technique, whereas the mechanical properties were measured by Vickers hardness testing, V-notched Charpy impact testing and tensile testing. The microscopy observations suggested a fully martensitic microstructure, whereas martensite was considerably finer in NiCrSi and NiCrMoV steels compared to MnCrB steel. Moreover, the NiCrSi and NiCrMoV steels showed significantly higher strengths and lower ductility than MnCrB steel. The results suggested that the small additions of alloying elements and different prior austenite grain sizes were mainly responsible for the observed microstructural and mechanical properties variations.

**Keywords:** Martensite-refinement, quench-hardening, medium carbon steel, microstructural characteristics, mechanical properties

## 1. Introduction

Severe working environments at different temperatures and loading conditions have risen the needs for steels with remarkably higher mechanical properties, e.g. high strengths, impact toughness, fracture toughness, fatigue resistance, hardness and wear resistance. As a solution, medium carbon steels with a martensitic or tempered-martensitic structure have been widely introduced by steel makers since about early 1980s and are extensively used in automotive, oil/gas and tool-making industries, e.g. [1,2,3,4]. In terms of microstructure, a fine lath martensite or tempered-martensite with

a high dislocation density and short free mean path in addition to nano-scale Fe/alloy carbide precipitates are mainly responsible for their mechanical properties [5,6]. However, in wear resistance tools further improvements to the strength and toughness of these steels are still sought, particularly to a better performance under severe working conditions [7].

The improvements have been mainly achieved by controlling and applying novel casting, thermomechanical and heat treatment processes, and also chemical composition of steels [8,9,10,11]. In this way, reducing the non-metallic inclusions and porosities, and increasing the homogeneity of chemical composition and microstructure, in particular prior austenite grain size, are mainly controlled through casting and thermomechanical processing. Moreover, a high strength martensitic structure of engineering components is manipulated by quenching-hardening and alloying additions [2,12,13,14]. The alloying additions mainly aim to improve the hardenability and final mechanical properties of steels. However, in alloy steels, a subsequent tempering process is usually required to increase the toughness, uniformity of microstructure and mechanical properties and to control the amount of retained austenite and Fe/alloy carbide precipitates and quenching-defects, and to reduce hydrogen embrittlement, e.g. [15,16,17,18,19].

Although these processes have been widely studied in the literature, no comparative research has focused on the as-quenched structure of quenched-tempered and quench-hardened low alloy medium carbon steels. It is well known that the final microstructure and mechanical properties of these steels are inherited from their parent martensite. The martensite structure is dependent upon several factors such as chemical composition, prior austenite grain size and cooling rate [20]. However, in low alloy medium carbon steels, it is hard to attribute the microstructure changes and difference in mechanical properties to any particular element due to small additions of alloying elements. Therefore, a systematic analysis was performed on three medium carbon steels with different alloying contents after quench-hardening from different temperatures to better understand the effect of chemical composition on microstructure and its relation to mechanical properties.

## 2. Experimental Procedure

The materials used in this investigation included three commercial hot rolled steels, received in fully annealed condition. These steels are especially designed to produce wear resistance tools which undergo a dominant impact/sliding wear. Table 1 compares the chemical compositions of investigated steels. The amount of each element

was determined using a spark Optical Emission Spectroscopy (OES) technique and are hereafter referred to as "MnCrB", "NiCrSi" and "NiCrMoV" steels. The MnCrB and NiCrSi steels were produced through electric arc melting, ladle arc melting and vacuum degassing, whereas the NiCrMoV steel was cast by Vacuum-Induction-Melting (VIM) and refined through Electro-Slag-Remelting (ESR). The NiCrSi and NiCrMoV steel are quenched-tempered steels (oil quenching and tempering), whereas MnCrB steel is a quenched-hardened steel (only water quenching). Generally, the NiCrSi and NiCrMoV steels are required to be tempered after quenching to minimise the risk of quench-cracking. Moreover, under similar working environments, the NiCrSi and NiCrMoV steels have a longer life time or better wear resistance compared to MnCrB steel.

**Table 1,** Chemical composition of investigated steels (wt%).

| Steel | C | Si | Mn | Cr | V | Mo | Ni | Ti | B | S | P | Fe |
|-------|------|------|------|------|------|------|------|-------|-------|-------|-------|------|
| MnCrB | 0.30 | 0.30 | 1.30 | 0.53 | - | - | - | 0.050 | 0.004 | 0.014 | 0.013 | Bal. |
| NiCrSi | 0.36 | 0.89 | 0.60 | 0.9 | - | 0.06 | 3.11 | - | - | 0.010 | - | Bal. |
| NiCrMoV | 0.50 | 0.22 | 0.65 | 1.33 | 0.52 | 0.77 | 3.70 | 0.002 | - | - | - | Bal. |

Samples with a size of 20×20×100 mm$^3$ were subjected to quench-hardening from different austenitisation temperatures and in water or oil mediums, assisted by agitation. All samples were held at austenitisation temperature for one hour per inch of ruling section. Austenitisation temperatures of 850, 900 and 950 °C were chosen for the hardening. Optimum austenitisation temperatures were applied to prepare samples for tensile and Charpy testing. However, our initial analysis showed an optimum temperature of 850 ºC for MnCrB and NiCrSi steels and 900 ºC for the NiCrMoV steel. The cooling rate during oil and water quenching was monitored by a Picolog recorder using a N-type thermocouple. Sample preparation for microstructural characterisations was performed according to standard methods on both rolling and normal direction planes. In addition, tensile and Charpy specimens were prepared from the rolling direction.

Microstructural characterisations were done by optical microscopy and Scanning Electron Microscopy (SEM) and energy dispersive X-ray spectroscopy (EDS) microanalysis using a FEG-Nova NanoSEM at 20 kV. The prior austenite grain boundaries were revealed using the oxidation etching technique [21] and the grain size was measured by linear intercept method according to ASTM E112.

The crystalline structure of the studied steels was characterised using a PANalytical Empyrean X-ray diffractometer with Co Kα radiation (i.e. including Co kα$_1$ (λ=0.178900nm) and Co kα$_2$ (λ=0.179284 nm) radiations) and with the power conditions of 40 kV and 40 mA. The retained austenite was characterised through Rietveld refinement using the Topas Academic package software V5.0. The X-Ray Diffraction (XRD) patterns were calibrated using a diffraction pattern of standard silicon sample (SRM 640e). The dislocation density was estimated according to Williamson–Hall (WH) method based on XRD data using the following equation [22]:

$$\text{Dislocation density} = 14.4(\varepsilon^2/b^2) \tag{1}$$

where ε and b are microstrain and Burger's vector (0.248 nm for ferrite), respectively. The microstrain was approximated using the equation below, using all diffraction peaks.

$$\delta(\cos\theta/\lambda) = \alpha + 2\varepsilon(\sin\theta/\lambda) \tag{2}$$

$$\alpha = 0.9/D \tag{3}$$

where δ, θ (radians), λ, α, ε and D are the physical broadening of XRD peak width (i.e. Full Width Half Maximum (FWHM)), diffraction angle, X-ray wavelength and average particle size, respectively.

The hardness property was determined by Vickers hardness testing (according to ASTM E92) with 30 kg load and 15 s holding time before unloading. The average hardness value was calculated from at least ten measurements for each sample. For the sake of comparison, HV hardness was converted to HRC according to ASTM E140.

The tensile properties of heat treated samples at optimum austenitisation temperature were determined according to ISO-6892 using a Zwick-Roell testing machine. The elongation during the test in cylindrical dog-bone shaped tensile specimens with a gauge length of 25 mm and gauge diameter of 5 mm was recorded by a non-contact high resolution laserXtens extensometer. The test was repeated three times using three separate samples from each steel to ensure the repeatability of tensile properties. The true stress-strain curves were converted from engineering stress-strain results according to standard procedure [23].

The impact toughness of steels was determined by V-notched Charpy impact testing using a pendulum Avery-Denison Charpy testing machine (a nominal energy of 300 J). Standard Charpy impact specimens with a size of 55×10×10 mm$^3$ and a notch radius of 0.25 mm were tested according to ASTM E23 at room temperature. The V-notch edge and front edge were parallel to transverse and normal directions, respectively. The test was repeated three times using three separate samples to check the repeatability of

results. Following the Charpy impact and tensile testing, the fractured samples were examined by SEM.

## 3. Results

### 3.1. Initial Microstructure

Fig. 1 shows optical and SEM micrographs corresponding to the microstructure of the as-received steels. The MnCrB steel consisted of pearlitic grains surrounded by allotriomorphic ferrite. The NiCrSi and NiCrMoV steels comprised lath shaped ferritic structure with dispersive carbide precipitates.
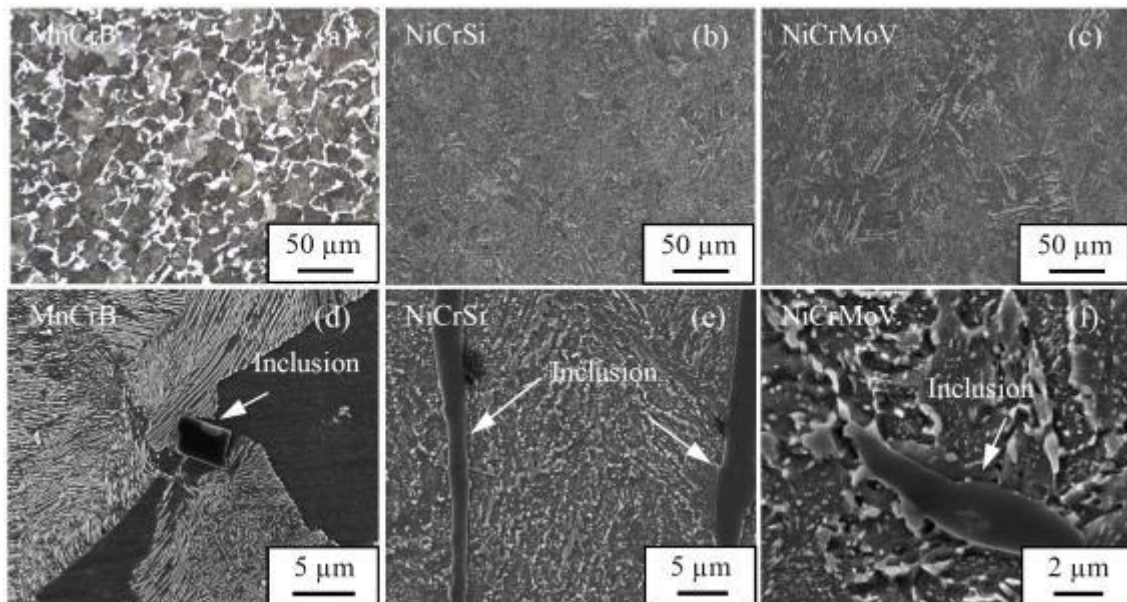


**Fig. 1,** Initial microstructure of studied steels, (a) to (c) optical micrographs, (d) to (f) SEM micrographs.

In addition, the non-metallic inclusions of the steels have been characterised for their densities, morphologies and chemical compositions (e.g. Figs. 1 ~~(g)~~ (d) to ~~(i)~~ (f)). The MnCrB and NiCrSi steels were found to contain inclusions of both elongated and equi-axed morphologies. The NiCrMoV steel was found to have equiaxial-shaped inclusions in its microstructure. SEM-EDS analysis of inclusions showed a large frequency of Mn-S and Ti rich inclusions in MnCrB steel and Mn-S inclusions in NiCrSi steel, whereas the majority of inclusions in NiCrMoV steel had a complex chemical composition and contain different metallic and non-metallic elements, e.g. Mn, V, Cr and S. Among the observed inclusions in NiCrVMo steel, the frequency of Mn, S and V containing inclusions was relatively high. The inclusions/micro-porosities were distributed non-uniformly and density of inclusions/micro-porosities was different at different regions

of samples. The average sizes of inclusions/micro-porosities were determined to be 27.1±17.0, 16.1±13.1 and 20.2±14.4 (µm) in the NiCrSi, MnCrB and NiCrMoV steels, respectively. Moreover, the density of inclusions was qualitatively higher in MnCrB and NiCrSi steels. This was attributed to the casting process of studied steels, as VIM-ESR process in NiCrMoV steel was believed to significantly reduce inclusions. However, the effect of inclusions on mechanical properties of steels will be further clarified in the following sections.

## 3.2. Microstructural Evolution during Hardening

Fig. 2 shows a few selected cooling curves in which the temperature has been plotted versus instantaneous cooling rate during the quenching stage. The water quenching (with an average cooling rate of 18 ºC/s) can be seen to have substantially higher cooling rate than the oil quenching (with an average cooling rate of 2-4 ºC/s).
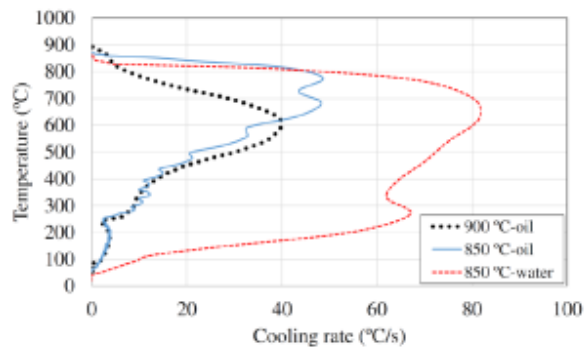


**Fig. 2,** Cooling rate versus temperature diagrams corresponding to samples quenched by water or oil at optimised austenitisation temperatures.

Fig. 3 shows SEM micrographs corresponding to the microstructure of as-quenched steels at different austenitisation temperatures, i.e. 850, 900 and 950 ºC. The microscopy analysis suggested a fully lath shaped martensitic structure throughout the cross sectional area in both rolling and normal directions of all samples. These micrographs are quite comparable to the results of other researchers in the literature, e.g. [24,25]. Furthermore, microscopy observations indicated that the initial microstructure was completely transformed to austenite during soaking time at all chosen austenitisation temperatures.

The martensite start temperature ($M_s$) in the MnCrB, NiCrSi and NiCrMoV steels was estimated as 361, 302 and 254 ºC, respectively [26]. As mentioned above, the cooling rate of water quenching was significantly larger than oil quenching, especially below 400 ºC, which is above the $M_s$ temperature. The relatively slower cooling rate during oil quenching could enhance auto-tempering in NiCrSi and NiCrMoV steels. However, it is clear that a maximum cooling rate of about 10 and 70 ºC/s, assisted by agitation, could secure full hardening in the NiCrSi/NiCrMoV and MnCrB steels, respectively (Fig. 2). In

this case, it is well known that the alloying additions (e.g. B, Cr, Ni, V and Mo) can considerably raise the hardenability of steels, e.g. [27,28,29,30]. However, our results demonstrated that the alloying additions might also affect the morphology of martensite.

Of particular note was that the martensitic structure of MnCrB steel in all conditions was significantly coarser (especially length) compared to NiCrSi and NiCrMoV steels (Fig. 3). Additionally, in MnCrB steel, microscopy observations suggested a significant increase in martensite length due to austenitisation at 950 ºC. However, SEM observations showed no meaningful difference in the morphology of martensite in NiCrSi and NiCrMoV steels due to austenitisation temperature increases.
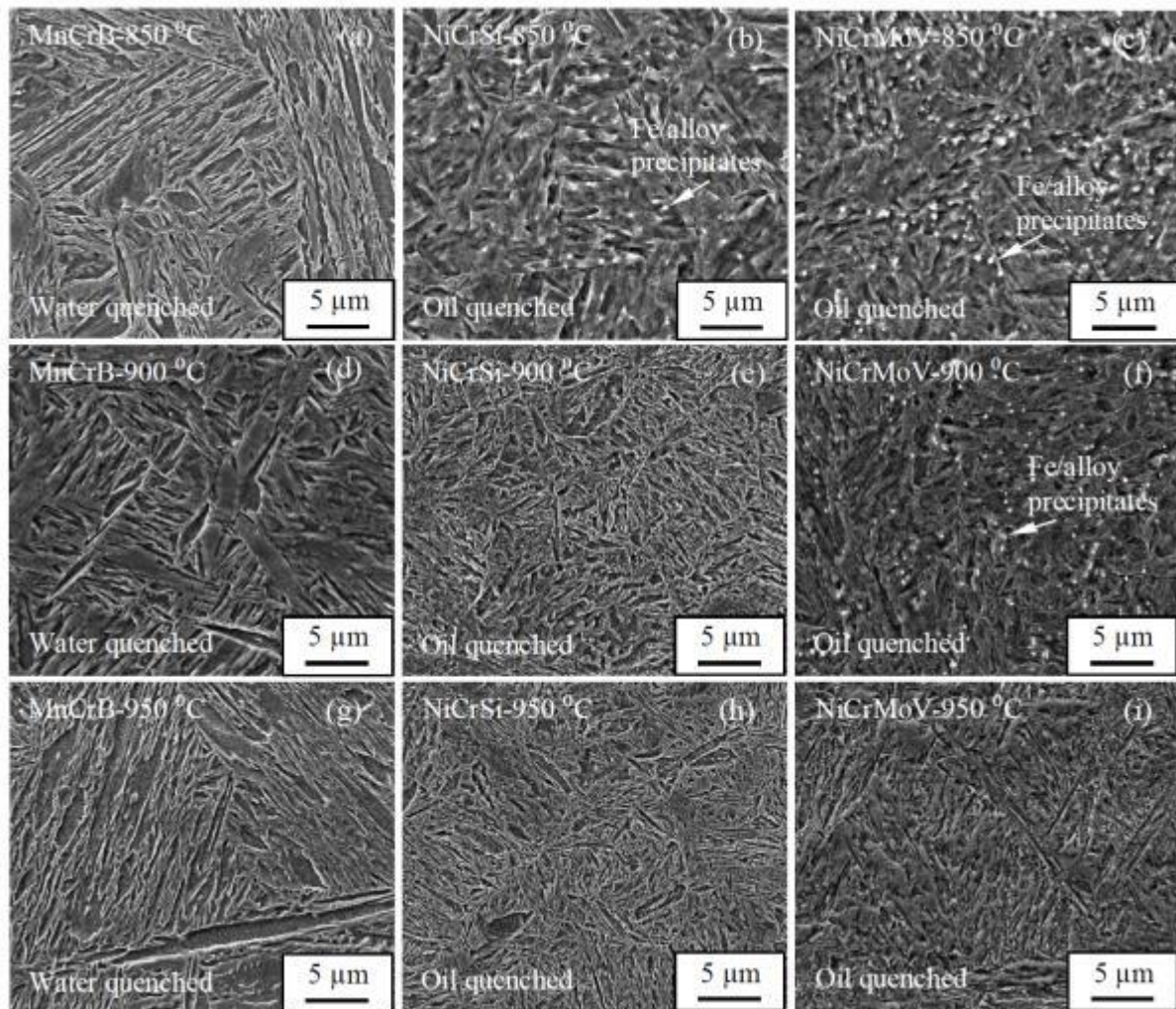


**Fig. 3,** SEM micrographs of quench-hardened samples at different austenitisation temperatures, i.e. 850, 900 and 950 ºC.

From the SEM analysis, it was also found that Fe/alloy carbide precipitates were present in NiCrSi and NiCrMoV steels (e.g. Figs. 3 (b) and (c) and (f)). Nevertheless, by

increasing the austenitisation temperature the density of these precipitates was qualitatively reduced. Coarse carbides might be formed during a growth-coarsening of undissolved/pre-existing precipitates or a rapid precipitation and growth/coarsening of newly formed precipitates. Moreover, the presence of nano-scale carbides inside the lath shaped ferritic constituents suggested that an auto-tempering might occur during quenching in all samples [31].

Fig. 4 shows typical non-metallic inclusions in SEM micrographs of as-quenched MnCrB, NiCrSi and NiCrMoV steels. Apart from the effects of sample preparation, the results occasionally demonstrated gap/decohesion at interfaces of inclusions and matrix in MnCrB steel. However, the gap/decohesion was frequently observed in NiCrSi and NiCrMoV steels, regardless of the chemical composition and morphology of inclusions. It should be noted that this behaviour was occasionally observed in the initial structure of all studied steels (e.g. Figs. 1 (d) to (f)).
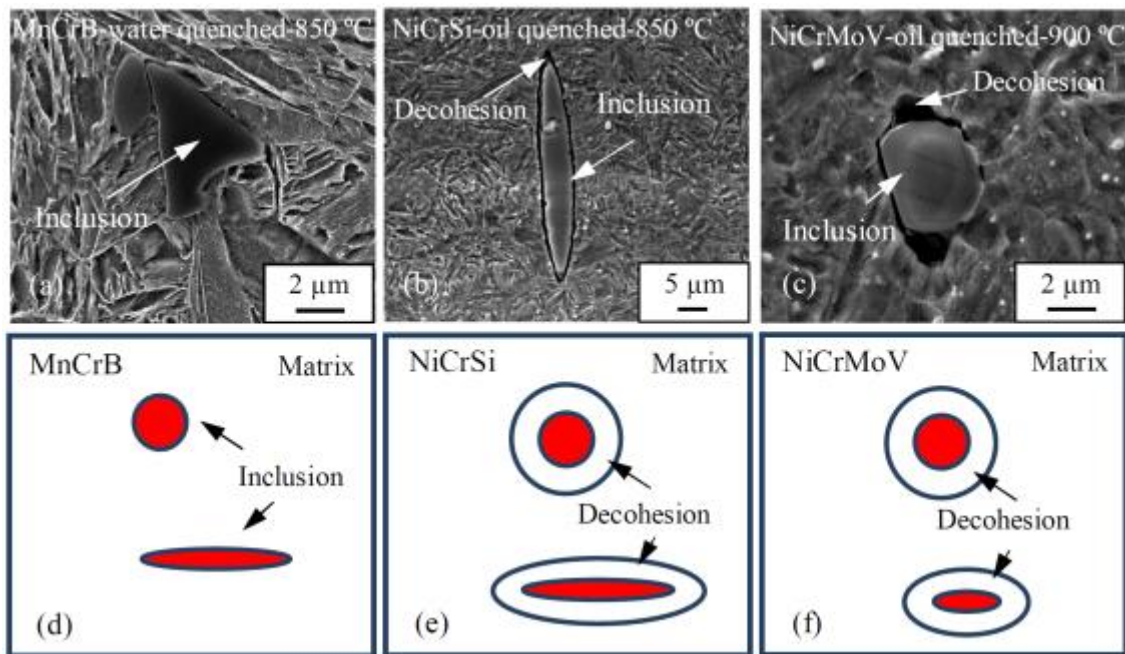


**Fig. 4,** (a) to (c) SEM micrographs, showing non-metallic inclusions in martensitic matrix, (d) to (f) Schematic illustration of inclusions, showing the position of gap/decohesion at interface of inclusions and matrix.

Fig. 5 (a) indicates a selected XRD spectrum of a quenched sample. The XRD analysis revealed the presence of retained austenite (FCC crystal-structure) and martensite (BCC-crystal structure [32]) in the as-quenched microstructure of three steels (Table 2). Further XRD analysis showed that the amount of retained austenite and its carbon content varied in terms of austenitisation temperature and type of steel. In MnCrB steel, the amount of retained austenite was considerably raised by increasing the

austenitisation temperature from 900 to 950 ºC, while both 850 and 900 ºC showed a similar level. In contrast, the level of retained austenite was rather similar in all austenitisation temperatures in NiCrSi and NiCrMoV steels.

The carbon content of retained austenite was measured from its lattice parameter (nm) using the following equation [33]:

$$a_{retained\ austenite} = 0.35467 + 0.00467\ wt\%\ C \tag{4}$$

From the XRD analysis, it was also found that the carbon content of retained austenite in MnCrB steel was relatively similar at all austenitisation temperatures. In contrast, in both NiCrSi and NiCrMoV steels, the carbon content of retained austenite was relatively raised at higher austenitisation temperatures.
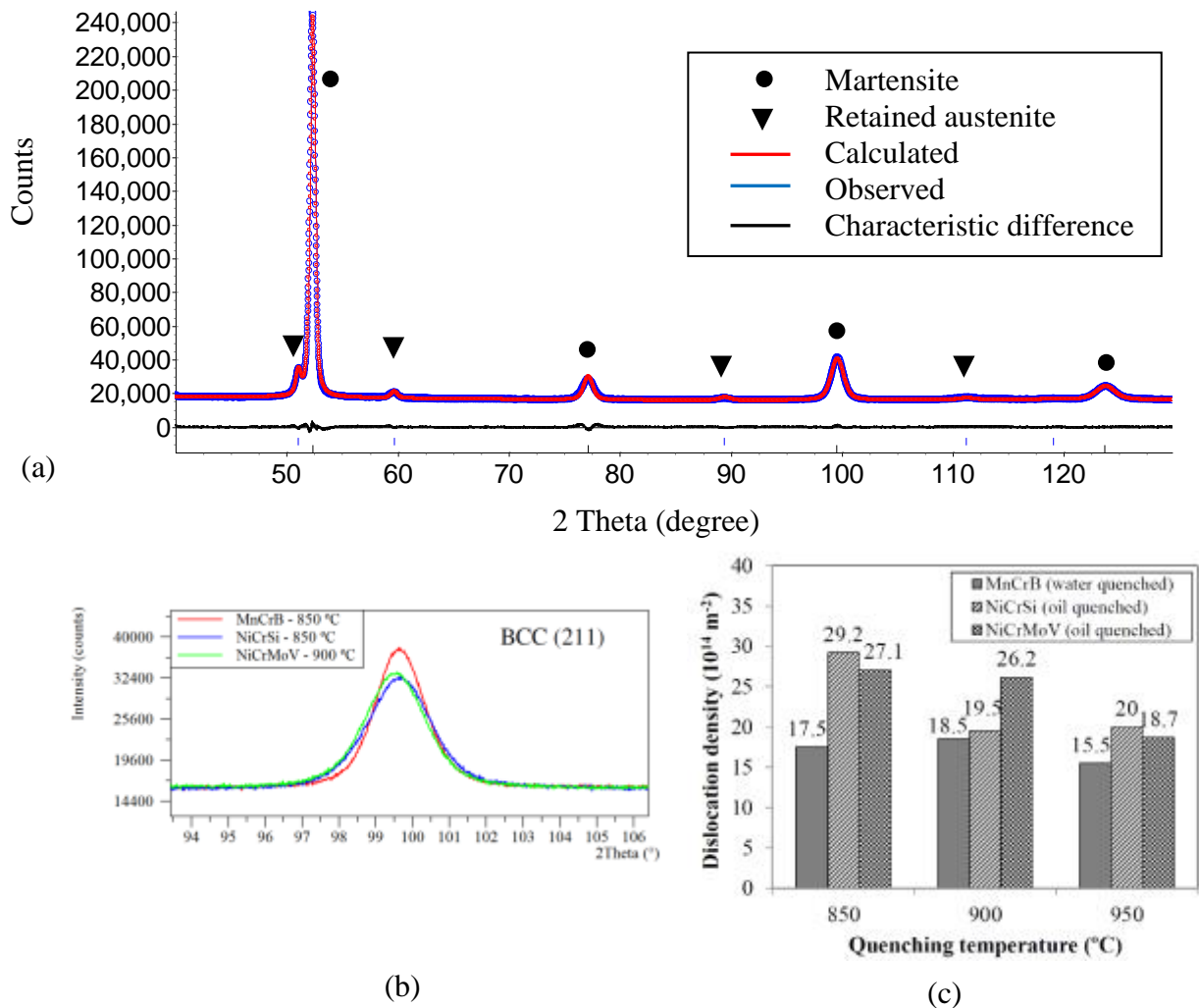


(a)



(b)



(c)

**Fig. 5,** (a) Typical XRD spectrum showing the presence of martensite and retained austenite, (b) A selected martensitic peak, showing broadening in NiCrSi and NiCrMoV steels compared to MnCrB steel, (c) Dislocation density, measured by WH method.

Fig. 5 (b) shows a selected XRD peak of studied steels (quenched at optimum austenitisation temperatures) so that the peaks of NiCrSi and NiCrMoV steels are considerably broader than MnCrB steel. Moreover, the XRD analysis exhibited a peak broadening as a function of austenitisation temperature. In fact, a broad martensite peak results from a higher carbon content, larger dislocation density and increased lattice micro-strain [5,22,34,35]. In MnCrB steel, the results suggested a very slight peak broadening at 850 and 900 ºC, while a considerable broadening was observed in NiCrSi steel at 850 ºC. A gradual peak broadening was also observed in NiCrMoV steel due to austenitisation temperature decreases.

Further XRD analysis showed the effect of austenitisation temperature on dislocation density of microstructure for each grade of steel (Fig. 5 (c)). The results are comparable to other reports in the literature about other grades of martensitic low/medium carbon steels [22,35,36,37]. It is clear that the dislocation density of NiCrSi and NiCrMoV steels was higher than MnCrB steel in all quenching conditions, especially at lower austenitisation temperatures. In MnCrB steel, the dislocation density was relatively similar in both austenitisation temperatures of 850 and 900 ºC, while it was slightly reduced at 950 ºC. It was also found that the dislocation density dramatically decreased at austenitisation temperatures of 900 ºC and 950 ºC in NiCrSi steel. However, a similar dislocation density was observed at austenitisation temperatures of 850 ºC and 900 ºC in NiCrMoV steel, while quenching at 950 ºC slightly decreased the dislocation density.

**Table 2**, The retained austenite characteristics determined by the XRD.

| Steel | $T_{Austenitisation}$ (ºC) | Retained austenite (vol%) | Carbon content (%) | Lattice parameter (nm) |
|---|---|---|---|---|
| MnCrB (water quenched) | 850 | 3.6 | 0.87 | 0.35874±0.00012 |
| | 900 | 4.1 | 0.84 | 0.35859±0.00015 |
| | 950 | 9.8 | 0.87 | 0.35876±0.00010 |
| NiCrSi (oil quenched) | 850 | 12.3 | 0.71 | 0.35800±0.00018 |
| | 900 | 14.9 | 1.07 | 0.35966±0.00009 |
| | 950 | 11.7 | 0.99 | 0.35931±0.00016 |
| NiCrMoV (oil quenched) | 850 | 8.8 | 0.90 | 0.35891±0.00017 |
| | 900 | 8.1 | 0.80 | 0.35841±0.00029 |
| | 950 | 8.3 | 1.08 | 0.39724±0.00014 |

Fig. 6 (a) shows the variation of prior austenite grain size as a function of austenitisation temperature. By increasing the temperature the average grain size was raised in all studied steels, though the growth rate seems to be different depending upon the grade of steel and temperature. In MnCrB steel, a dramatic growth/coarsening

was appeared at each temperature, whereas NiCrSi and NiCrMoV showed lower growth/coarsening rate, particularly from 850 to 900 °C. These results are consistent with the findings of other researchers who also reported prior austenite grain size increases in 300M steel due to a higher austenitisation temperature, e.g. from 850 to 1050 °C [38].
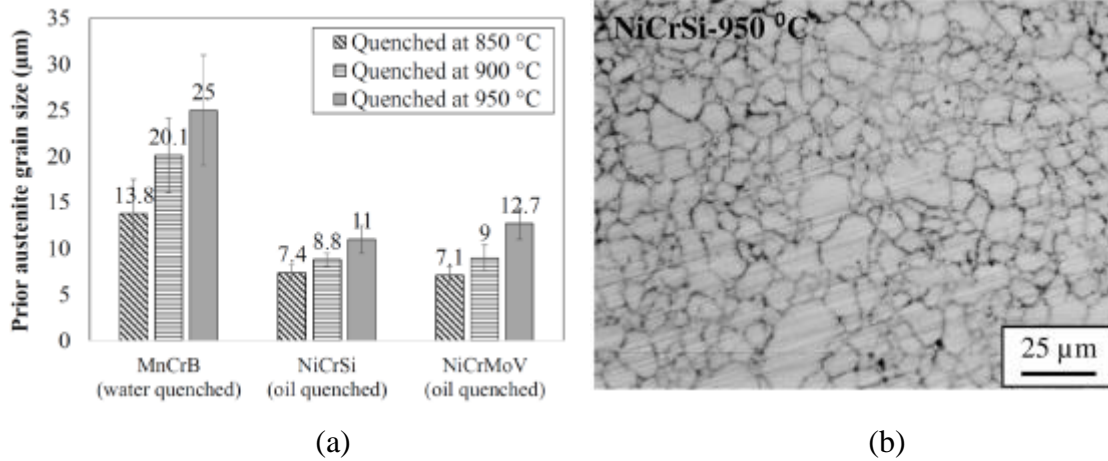


(a)                                                    (b)

**Fig. 6,** (a) Average prior austenite grain size, (b) A selected optical micrograph showing the prior austenite grain boundaries in NiCrSi steel after oxidation etching.

### 3.3. Mechanical Properties

Fig. 7 shows the hardness properties of studied steels. After quenching at 850 ºC, the MnCrB steel exhibited a hardness value of 55 HRC, whereas the other two grades showed a higher hardness, i.e. ~58-59 HRC. It was also found that a higher austenitisation temperature often led to the softening of all steels. The MnCrB steel was less sensitive to austenitisation temperature, whereas NiCrSi and NiCrMoV showed a more hardness reduction at higher austenitisation temperatures. Additionally, the results indicated no hardness reduction in NiCrMoV steel due to hardening at 900 ºC.
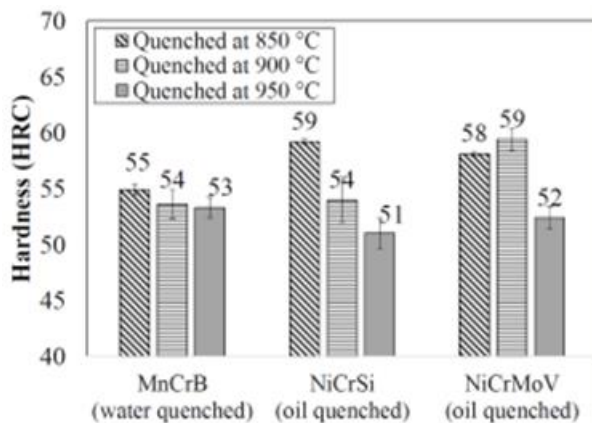


**Fig. 7,** Average hardness of as-quenched samples at different austenitisation temperatures.

Fig. 8 compares the V-notched Chrapy impact toughness of MnCrB, NiCrSi and NiCrMoV steels after quenching from optimum austenitisation temperatures. The results suggested a rather higher toughness in MnCrB steel compared to other steels.

Fig. 9 presents the tensile properties of MnCrB, NiCrSi and NiCrMoV steels after quenching from optimum austenitisation temperatures. The true stress-strain curves (Fig. 9 (a)) were plotted up to Ultimate Tensile Strength (UTS). It is clear that the yield strength of both the NiCrSi and NiCrMoV steels was higher than the MnCrB steel. Moreover, the results evidenced significantly higher UTS values and uniform elongation in NiCrSi and NiCrMoV steels compared to MnCrB steel. It was also found that the work hardening rate ($d\sigma/d\varepsilon$) during uniform elongation of NiCrSi and NiCrMoV steels was similar to each other and higher than MnCrB steel (Fig. 9 (b)). These results also indicate that NiCrSi and NiCrMoV steels are work hardened at lower level of plastic strains compared to MnCrB steel. However, as shown in Fig. 9 (c), the non-uniform elongation of NiCrSi and NiCrMoV steels was considerably lower than the MnCrB steel.
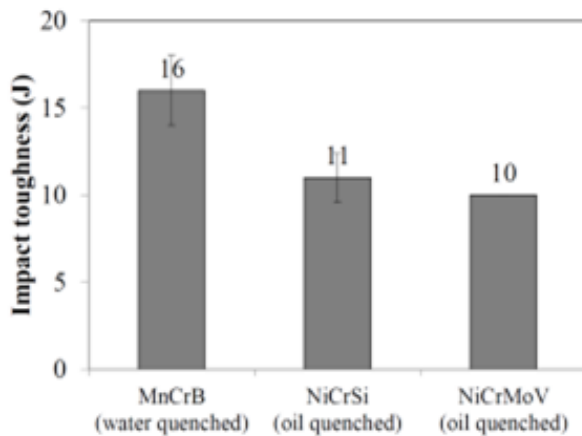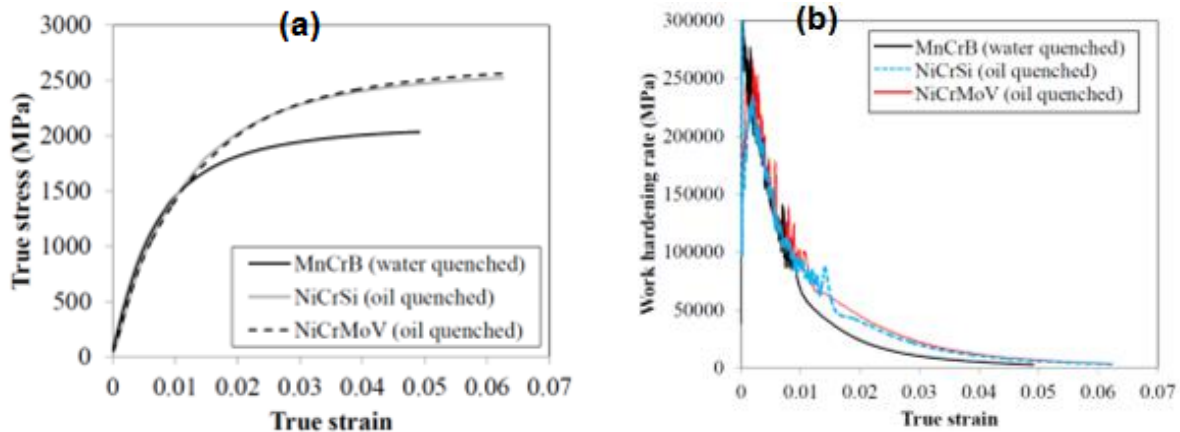


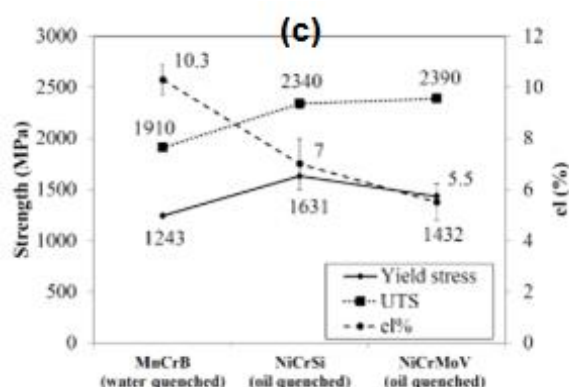**Fig. 8,** Average Charpy impact toughness.

**Fig. 9,** (a) and (b) Selected true stress–strain curves and corresponding strain hardening versus true strain curves, respectively, (c) Trend of yield strength, UTS and elongation variations, measured from engineering stress-strain.

## 3.4. Fractography of Fractured Specimens

Fig. 10 shows the fracture surface of Charpy specimens. A visual inspection of fracture surface suggested a rather similar cleavage to shear lip area ratio in all samples, i.e. ~50% (Figs. 10 (a) to (c)). It is well known that a higher energy per unit area is required to fracture the shear lip than cleavage area. It is thus clear that a similar level of Charpy energy was applied to fracture all specimens. Further analysis of fracture surfaces using SEM revealed a dominant dimple fracture feature in all steels. These results are consistent with impact strength results (Fig. 8), confirming a rather ductile fracture in all samples. However, from the SEM analysis, it was also found that the size and depth of dimples in the cleavage and shear lip areas of MnCrB steel were larger compared to NiCrSi and NiCrMoV steels.
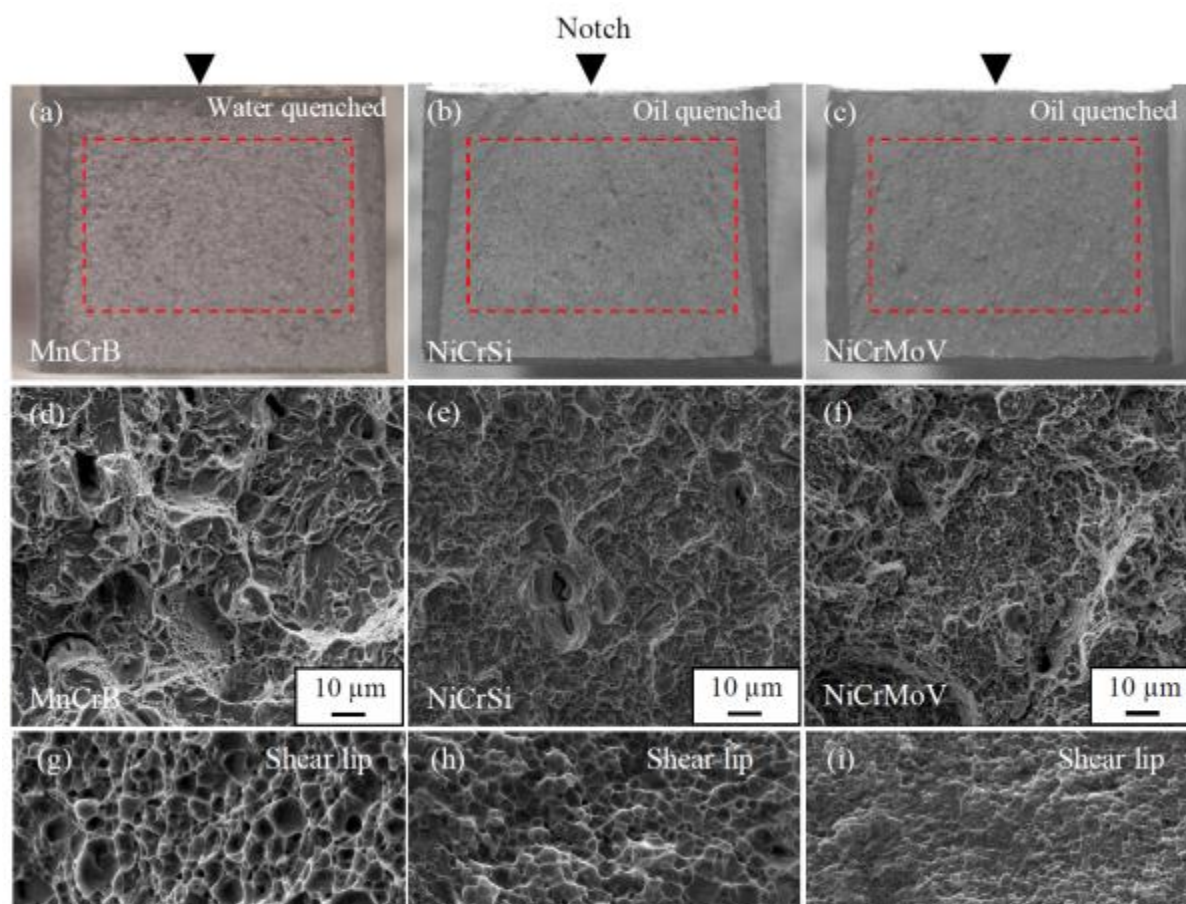
Fig. 11 compares the facture surface of some tensile specimens. A cup-and-cone fracture surface was appeared in all samples. As with Charpy specimens, a dominant dimple fracture surface was observed in all tensile specimens. The SEM microscopy also showed that the size and depth of dimples were relatively larger in MnCrB steel compared to NiCrSi and NiCrMoV steels.
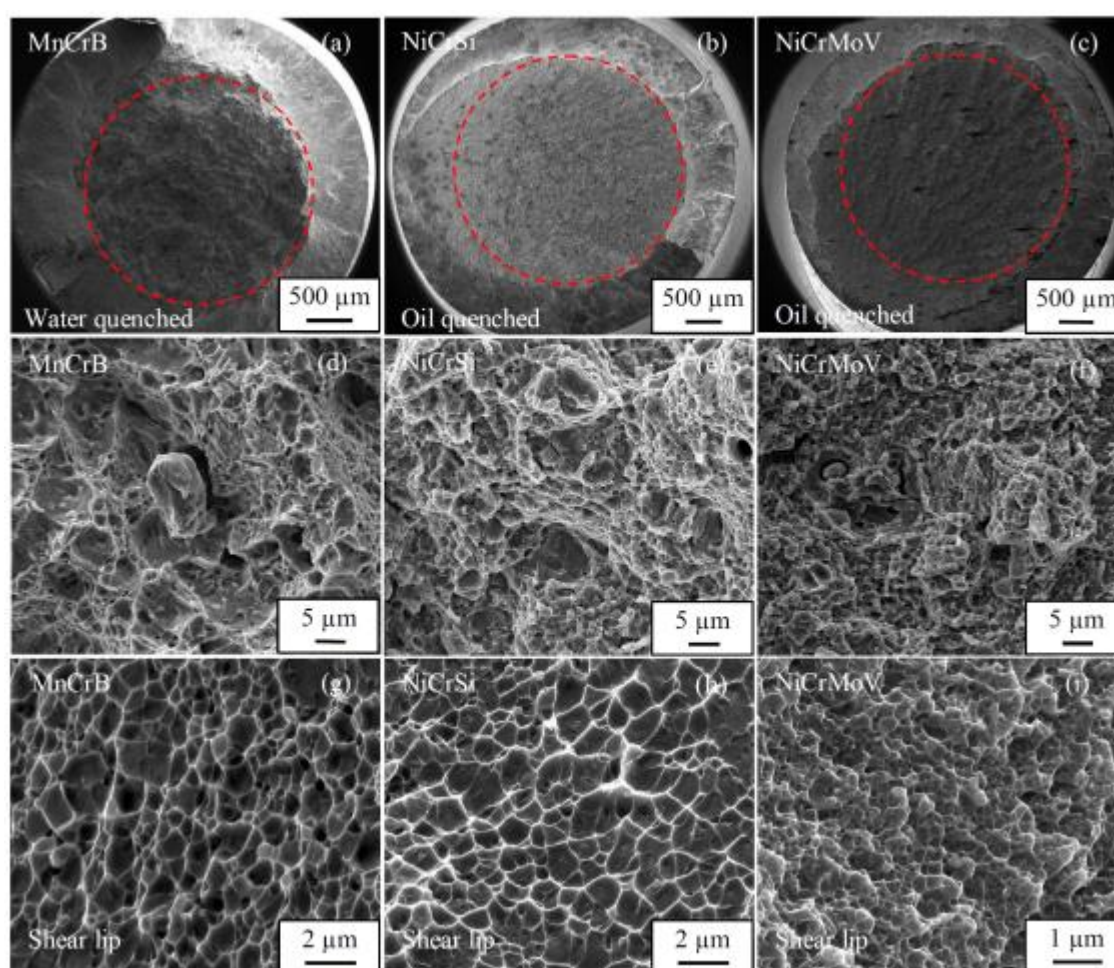


**Fig. 11,** (a) to (c) SEM micrographs corresponding to the fracture surface of tensile specimens, showing a cup-and-cone fracture surface, (d) to (f) SEM micrographs corresponding to the inside of red dashed circle in (a) to (c), (g) to (i) SEM micrographs corresponding to the shear lip area of fracture surface in (a) to (c).

## 4. Discussion

### 4.1. Prior Austenite

In MnCrB steel, the prior austenite grain size was considerably raised with increased austenitisation temperature, while this behaviour was rather sluggish in NiCrSi and NiCrMoV steels. In MnCrB steel, the austenite was expected to initially form from features with a high carbon concentration such as pearlitic regions [39,40]. Clearly, the size of pearlite colonies could act as a significant role in the final prior austenite grain size (Fig. 1). On the other hand, the austenite formation in NiCrSi and NiCrMoV steels was thought to be dominantly influenced by prior austenite grain size and the size of sub-grains with the same crystal orientation inside prior austenite grains [41,42]. In addition, the presence of V-carbide precipitates in NiCrMoV steel with a relatively high temperature stability could retard the growth/coarsening rate of austenite during the soaking time [40,43,44,45]. However, our results evidenced that the trend of prior austenite grain size variations was rather similar between NiCrSi and NiCrMoV steels. It is thus clear that the observed difference was primarily affected by the initial structure. This is consistent with other reports in the literature [41,46,47,48], suggesting that the initial structure can considerably affect the prior austenite grain size during hardening process.

Moreover, the results showed that the prior austenite grain size of NiCrSi and NiCrMoV steels was rather finer compared to MnCrB steel (Fig. 6). A finer prior austenite grain size could presumably encourage a finer martensite packet/block size and consequently generate a greater dislocation density through the microstructure during quenching [5,49,50]. This will be further clarified in the following sections.

### 4.2. Martensite

SEM analysis of all quenched samples showed that the martensite structure was significantly finer in both NiCrSi and NiCrMoV steels compared to MnCrB steel (Fig. 3). The refinement of martensite is a favourable structure to the mechanical properties, e.g. high strength, fracture toughness, fatigue resistance, hardness and wear resistance [5,50,51]. A possible explanation of this phenomenon is inferred by taking into consideration the effect of prior austenite grain size [24]. A finer prior austenite grain size of NiCrSi and NiCrMoV steels enhanced the refinement of martensite during quenching. Furthermore, a comparative analysis of results demonstrated that the prior

austenite grain size of NiCrSi and NiCrMoV steels after quenching at 950 °C was rather close to the prior austenite grain size of MnCrB steels at 850 °C. However, SEM observations demonstrated that the martensite in both NiCrSi and NiCrMoV steels was still finer than MnCrB steel. It has also been widely accepted that a higher cooling rate can enhance martensite refinement. In contrast, our results showed that the martensite was finer in NiCrSi and NiCrMoV steels in all conditions even after oil quenching with a considerably slower cooling rate (e.g. Fig. 2). The results point to the fact that a combination of solid solution strengthening and a finer prior austenite grain size might cause the martensite refinement. In a wider sense, finer prior austenite grain size in addition to solid solution strengthening, especially a higher carbon content, could increase local elastic energy which could auto-catalytically increase nucleation sites for new martensite plates in NiCrSi and NiCrMoV steels [5,50,52,53].

## 4.3. Non-metallic Inclusions

SEM observations frequently evidenced gap/decohesion at interfaces of inclusions and matrix in NiCrSi and NiCrMoV steels, while this behaviour was occasionally observed in MnCrB steel (Fig. 4). Decohesion between inclusions and matrix has been well studied by other researchers in the literature, e.g. [54]. It has been established that decohesion mainly results from the difference in the thermal expansion coefficients between inclusions and matrix and also a highly dislocated structure with a high level of transformational/thermal stresses during quenching can encourage this behaviour. According to microscopy observations, this effect was mainly ascribed to the remarkably finer martensitic structure of NiCrSi and NiCrMoV steels. In fact, a higher level of transformational stresses and a greater mismatch between inclusions and matrix might be generated which enhanced decohesion at interfaces. Furthermore, SEM-EDS analysis of inclusions in NiCrMoV steel revealed a high frequency of Mn, Cr, V and S containing inclusions, while the majority of inclusions in MnCrB and NiCrSi steels were rich only in Mn-S. Although there is no available data on the thermal expansion of inclusions, it is thought that a possible difference between thermal expansion of inclusions and matrix in NiCrMoV, NiCrSi and MnCrB steels was less likely the reason for the observed phenomenon. Further investigations into the thermal expansion coefficient and coherency of inclusions would be required to better understand this behaviour.

## 4.4. Retained Austenite

The XRD analysis showed no meaningful difference in the amount of retained austenite between NiCrSi and NiCrMoV steels due to different austenitisation temperatures. It was also found that the amount of retained austenite in NiCrSi and NiCrMoV steels was relatively higher than MnCrB steel. There are several factors which can influence the

amount of retained austenite in martensitic steels such as prior austenite grain size and chemical composition. It has been generally accepted that a smaller prior austenite grain size and alloying additions, especially carbon content, can reduce $M_s$ and consequently increase the retained austenite volume fraction [55]. However, the XRD results showed insignificant difference in the amount of retained austenite due to prior grain size variations in NiCrSi and NiCrMoV steels. It is thus inferred that the main reason for the observed difference was primarily attributed to the chemical composition of studied steels, particularly their carbon content.

The results also showed that the retained austenite in MnCrB steel was considerably raised after hardening at 950 ºC. Similarly, other researchers have reported a similar behaviour in other steels due to hardening at high temperatures, e.g. [56]. Microscopy observations revealed a considerable coarsening (Ostwald ripening) of prior austenite grains at 950 ºC. Further microscopy observations presented long martensite lath, crossing the whole grain interior of some prior austenite grains. As during coarsening the larger grains are coarsened at the expense of finer grain, a partial coarsening can leave fine grains in the microstructure. According to microscopy observations, it can be therefore inferred that a higher volume fraction of austenite was retained within the remaining fine austenite grains. Moreover, a further dissolution of Fe/alloy carbide precipitates due to a higher austenitisation temperature could increase carbon atoms in solution which might increase the stabilisation of austenite against martensite transformation.

## 4.5. Mechanical Properties

The present paper reports on the tensile and Charpy impact properties of studied steels, quenched from optimum austenitisation temperatures, i.e. 900 and 850 °C for NiCrMoV and NiCrSi/MnCrB steels, respectively. According to hardness results and microscopy observations, these temperatures were selected to minimise prior austenite growth/coarsening and to maximise the dissolution/homogenisation of alloying elements in the microstructure [5,57].

### 4.5.1. Yield Strength and Hardness

From hardness analysis, it was found that the average hardness can reach up to ~59 HRC in NiCrSi and NiCrMoV steels after oil quenching, while MnCrB steel gives a maximum hardness of about 55HRC after water quenching (Fig. 7). A similar trend was observed in the yield strength of studied steels (Fig. 9). The yield strength of NiCrSi and NiCrMoV steels was quite similar and significantly greater than MnCrB steel. It has been well established that the strength of martensitic structure is proportional to the friction stress (pure Fe), solid solution strengthening from alloying elements (e.g. Mn and Ni),

martensite lath width, martensite packet/block size and dislocation density [5,52]. The friction stress is strongly dependent on the crystal structure and chemical composition of steel and it was assumed that it was the same in the studied steel due to a small amount of alloying additions [58,59]. Therefore, the effects of latter items were taken into consideration to interpret the observed differences. From the microscopy observations, it was found that NiCrSi and NiCrMoV steels have a rather finer lath martensite and prior austenite grain size than MnCrB steel (Figs. 3 and 6). By increasing the austenitisation temperature the hardness of all samples was generally reduced. As mentioned above, the prior austenite grain size was raised by increasing the austenitisation temperature. According to the Hall-petch relationship, smaller grains with high angle boundaries can increase strength of steel. In fact, dislocations are piled up behind high angle boundaries during deformation, increasing the strength of material [52]. Moreover, it has been established that a larger prior austenite grain can form coarser martensite packets/blocks with a lower dislocation density after quenching which reduces the strengthening effect of martensite [60,61,62]. In this case, the XRD results also showed a lower dislocation density in MnCrB steel compared to NiCrSi and NiCrMoV steels (Fig. 5 (c)). The solid solution strengthening of alloying additions, especially carbon, could be another reason for the higher strength of NiCrSi and NiCrMoV steels. However, possible precipitation and growth-coarsening of Fe/alloy carbide precipitates, in particular V-carbides, would have lowered the free carbon atoms in solute and reduce the carbon solid solution strengthening in NiCrMoV steel. It is thus clear that the observed difference in the microstructure of steels and alloying additions were mainly responsible for the different yield-strength/hardness of steels after quenching. This is consistent with other reports in the literature, suggesting that a finer prior austenite grain size, higher dislocation density of lath martensite and solid solution could considerably contribute in strengthening of martensitic steels [50,63].

### 4.5.2. Work Hardening Rate and Elongation

A rather similar work hardening rate was observed during uniform elongation in the NiCrSi and NiCrMoV steels, while it was higher than the work hardening rate of MnCrB steel (Fig. 9 (b)). It has been reported in the literature that the work hardening rate of lath martensite at room temperature during uniform elongation can be considerably raised by carbon content, dislocation density and also Transformation Induced Plasticity (TRIP) effect of retained austenite [37,59]. The results also suggested a higher uniform elongation in NiCrSi and NiCrMoV steels than MnCrB steel. As the amount of retained austenite was significantly high in NiCrSi and NiCrMoV steels, it is thought that the higher work hardening rate was strongly influenced by TRIP effect. A gradual transformation of retained austenite during plastic deformation increased the work

hardening rate and uniform elongation [33]. Moreover, a higher dislocation density and carbon content of NiCrSi and NiCrMoV steels compared to MnCrB steel was considered to be another reason for the higher work hardening rate during tensile deformation (Fig. 5 (c)). These results are in agreement with the findings of other researchers in the literature who also reported a similar behaviour in lath martensitic steels [37].

The tensile results also showed that the non-uniform elongation of MnCrB steel was significantly larger than NiCrSi and NiCrMoV steels. This phenomenon was explained based on two reasons. First of all, dislocations can act as crack initiation site in a dimple fracture mode. In this case, rather fine dimples with a shallow depth in the fracture surface of NiCrSi and NiCrMoV steels suggested  more nucleation sites for void formation (Fig. 11) [64,65]. Clearly, a finer martensitic structure with a higher dislocation density in NiCrSi and NiCrMoV steels could accelerate crack initiation, lowering non-uniform elongation [64]. Moreover, the observed decohesion at interface of inclusions and matrix in NiCrSi and NiCrMoV steels could encourage crack initiation during non-uniform elongation, reducing the non-uniform elongation (e.g. Fig. 4) [65].

### 4.5.3. Impact Toughness

The results suggested similar toughness in NiCrSi and NiCrMoV steels, while it was slightly lower than MnCrB steel. From the fractography analysis, it was also found that a ductile fracture mode was dominant in all samples (Fig. 10). It is well known that a finer prior austenite grain size and subsequently finer packet/block martensite size as well as TRIP effect of retained austenite can improve the impact toughness of martensitic steels [60,66,67]. On the other hand, a higher carbon content of steel and also non-metallic inclusions can considerably lower the impact toughness of steels. The high angle boundaries can more effectively deflect the crack propagation, increasing the absorbed energy during impact toughness. Moreover, a possible TRIP effect of retained austenite during plastic deformation can relieve local stress concentration and delay micro-crack initiation. Additionally, during crack propagation, a high stress concentration at the tip of crack can enhance the TRIP effect of retained austenite. This releases the stress concentration and energy of crack tip and consequently suppresses the crack propagation. However, our results showed a reverse behaviour in studied steels, precluding the effect of prior austenite grain size and retained austenite on the impact toughness (Figs. 6 and 8 and Table 2). It is thus inferred that a lower amount of carbon content was ~~most~~ likely the reason for the higher toughness of MnCrB steel. Additionally, the observed decohesion at the interface of inclusions and martensitic matrix in NiCrSi and NiCrMoV steels could enhance crack initiation and reduce their impact toughness. The results also showed relatively finer dimple features in the fracture surface of NiCrSi and NiCrMoV steels which might result from the effect of

dislocation density (Fig. 10). Perhaps a relatively higher dislocation density encouraged more void formation.

## 5. Conclusions

1) A considerable martensite refinement was observed in NiCrSi and NiCrMoV steels compared to MnCrB steel, regardless of prior austenite grain size and cooling rate. Moreover, the results also suggested a higher dislocation density in NiCrSi and NiCrMoV steels. These were mainly attributed to the effect of alloying additions.

2) The results suggested that the small additions of alloying elements, especially carbon content, finer prior austenite grain size and higher dislocation density considerably contributed in strengthening of NiCrSi and NiCrMoV steels.

3) V-notched Charpy impact toughness of NiCrSi and NiCrMoV steels was rather similar, though it was relatively lower than the toughness of MnCrB steel. The observed difference was primarily attributed to the non-metallic inclusions and chemical composition of steels, especially a higher carbon content of NiCrSi and NiCrMoV steels.

4) In NiCrSi and NiCrMoV steels, the retained austenite volume fraction was significantly higher than MnCrB steel. This was mainly ascribed to the effect of alloying additions, in particular carbon content. It was also found that the observed retained austenite might increase the work hardening rate and uniform elongation of NiCrSi and NiCrMoV steels due to the TRIP effect.

5) Decohesion at interfaces of inclusions and martensitic matrix was frequently appeared in NiCrSi and NiCrMoV steels, while this behaviour was occasionally observed in MnCrB steel. The results suggested that the degree of interface decohesion between the martensite matrix and inclusions increased as the strength of martensite increased.

## Acknowledgment

## References

[1]  G.Roberts, G.Krauss, and R.Kennedy, *Tool Steels*. ASM International, 1998.

[2]  G.Krauss, "Deformation and Fracture in Martensitic Carbon Steels Tempered at Low Temperatures,"

*Metallurgical and Materials Transcations A*, vol. 32A, pp. 861-877, 2001.

[3]   R.J.Tunney and N.Ridley, "Tempering of High Purity and Commercially Based Steels Containing 10 wt-% Tungsten or 5 wt-% Molybdenum," *Metal Science*, vol. 13, no. 10, pp. 585-590, 1979.

[4]   Y.Tomita and T.Okawa, "Effect of Microstructure on Mechanical Properties of Isothermally Bainite Transformmed 300M Steel," *Materials Science and Engineering A*, vol. 172, pp. 145-151, 1993.

[5]   G.Krauss, "Martensite in Steel: Strength and Structure," *Materials Science and Engineering A* , vol. 273-275, pp. 40-57, 1999.

[6]   A.Schremb, "Steel Alloy," Patent US20120000336 A1, Jan. 5, 2012.

[7]   E.Abbasi, Q.Luo, and D.Owens, "Case Study: Wear Mechanisms of NiCrVMo-steel and CrB-steel Scrap Shear Blades," *Wear*, vol. 398-399, pp. 29-40, 2018.

[8]   R.Schlatter, "Vacuum Induction Melting," *Journal of Metals*, vol. 24, no. 5, pp. 17-25, 1972.

[9]   K.A.Ridal, P.F.Morris, A.S.Normanton, and A.Scholes, "Effect of Melting, Refining and Casting on Product Quality and Properties," *Ironmaking and Steelmaking*, vol. 34, no. 6, pp. 449-457, 2007.

[10]  E.Abbasi, "Processing and Structure of High Strength Steels," PhD Thesis, The University of Sheffield, Sheffield, 2015.

[11]  M.G.Hebsur, "Improved Fracture Toughness and Resistance to Fatigue Crack Propagation in ESR Steels," *Canadian Metallurgical Quarterly*, vol. 20, no. 4, pp. 437-447, 1981.

[12]  D.V.Edmonds, et al., "Quenching and Partitioning Martensite—A Novel Steel Heat Treatment," *Materials Science and Engineering: A*, vol. 438–440, pp. 25-34, 2006.

[13]  L.C.F.Canale, G.E.Totten, and R.A.Mesquita, *Failure Analysis of Heat Treated Steel Components*. ASM International, 2008.

[14]  Y.Tomita, "Development of Fracture Toughness of Ultrahigh Strength, Medium Carbon, Low Alloy Steels for Aerospace Applications," *International Materials Reviews*, vol. 45, no. 1, pp. 27-37, 2000.

[15]  M.Hunkel, et al., "Size Change due to Anisotropic Dilation Behaviour of Low Alloy SAE 5120 Steel," *Materials Technology*, vol. 78, pp. 45-51, 2007.

[16]  Y.Toshioka, "Heat Treatment Deformation of Steel Products," *Materials Science and Technology*, vol. 1, no. 10, pp. 883-892, 1985.

[17]  W.Sh.Lee and T.T.Su, "Mechanical Properties and Microstructural Features of AISI 4340 High-strength Alloy Steel under Quenched and Tempered Conditions," *Journal of Materials Processing Technology*, vol. 87, pp. 198-206, 1999.

[18]  X.Luo and G.E.Totten, "Analysis and Prevention of Quenching Failures and Proper Selection of Quenching Media: An Overview," *Journal of ASTM International*, vol. 8, no. 4, pp. 1-29, 2011.

[19]  H.K.D.H.Bhadeshia, "Prevention of Hydrogen Embrittlement in Steels," *ISIJ International*, vol. 56, no. 1, p. 24–36, 2016.

[20]  E.Pereloma and D.V.Edmonds, *Phase Transformations in Steels*. Elsevier Science & Technology, 2012, vol. 2.

[21]  R.Riedl, "The Determination of Austenite Grain Size in Ferrous Metals," *Metallography*, vol. 14, pp. 119-128, 1981.

[22] Sh.Takebayashi, T.Kunieda, N.Yoshinaga, K.Ushioda, and Sh.Ogata, "Comparison of the Dislocation Density in Martensitic Steels Evaluated by Some X-ray Diffraction Methods," *ISIJ International*, vol. 50, no. 6, p. 875–882, 2010.

[23] J.R.Davis, *Tensile Testing*, 2nd ed. ASM International, 2004.

[24] S.Morito, H.Tanaka, R.Konishi, T.Furuhara, and T.Maki, "The Morphology and Crystallography of Lath Martensite in Fe-C Alloys," *Acta Materialia*, vol. 51, no. 6, pp. 1789-1799, 2003.

[25] A.Shibata, S.Morito, T.Furuhara, and T.Maki, "Substructures of Lenticular Martensites with Different Martensite Start Temperatures in Ferrous Alloys," *Acta Materialia*, vol. 57, pp. 483-492, 2009.

[26] D.Barbier, "Extension of the Martensite Transformation Temperature Relation to Larger Alloying Elements and Contents," *Advanced Engineering Materials*, vol. 14, no. 1, pp. 122-127, 2016.

[27] X.Tingdong, S.Shenhua, Y.Zhexi, and Y.Zongsen, "Two Types of Boron Segregation at Austenite Grain Boundaries and Their Mutual Relation," *Journal of Materials Science*, vol. 25, pp. 1739-1744, 1990.

[28] L.Lanier, G.Metauer, and M.Moukassi, "Microprecipitation in Boron-Containing High-Carbon Steels," *Mikrochimica Acta*, vol. 114-115, pp. 353-361, 1994.

[29] M.Ch.Somani, D.A.Porter, P.Karjalainen, T.Rasmus, and M.Hirvi, "Method for Manufacturing a High Strength Structural Steel and a High Strength Structural Steel Product," Patent US 2014/0299237 A1, Oct. 9, 2014.

[30] G.E.Totten, C.E.Bates, and N.A.Clinton, *Handbook of Quenchants and Quenching Technology*. ASM International, 1993.

[31] D.Kim, S.J.Lee, and B.C.D.Cooman, "Microstructure of Low C Steel Isothermally Transformed in the Ms to Mf Temperature Range," *Metallurgical and Materials Transactions A*, vol. 43A, pp. 4967-4983, 2012.

[32] B.Hutchinson, et al., "Microstructures and Hardness of As-quenched Martensites (0.1–0.5%C)," *Acta Materialia*, vol. 59, no. 14, pp. 5845-5858, 2011.

[33] E.Abbasi and W.M.Rainforth, "Microstructural Evolution during Bainite Transformation in a Vanadium Microalloyed TRIP-assisted Steel," *Materials Science & Engineering A*, vol. 651, pp. 822-830, 2016.

[34] A.R.Stokes and A.J.C.Wilson, "A Method of Calculating the Integral Breadths of Debye-Scherrer Lines," *Mathematical Proceedings of the Cambridge Philosophical Society*, vol. 38, no. 3, pp. 313-322, 1942.

[35] F.HajyAkbary, J.Sietsma, A.J.Böttger, and M.J.Santofimia, "An Improved X-ray Diffraction Analysis Method to Characterize Dislocation Density in Lath Martensitic Structures," *Materials Science & Engineering A*, vol. 639, pp. 208-218, 2015.

[36] T.Kunieda, M.Nakai, Y.Murata, T.Koyama, and M.Morinaga, "Estimation of the System Free Energy of Martensite Phase in an Fe-Cr-C Ternary Alloy," *ISIJ International*, vol. 45, no. 12, pp. 1909-1914, 2005.

[37] K.O.Findley, J.Hidalgo, R.M.Huizenga, and M.J.Santofimia, "Controlling the Work Hardening of Martensite to Increase the Strength/ductility Balance in Quenched and Partitioned Steels," *Materials and Design*, vol. 117, p. 248–256, 2017.

[38] S.S.Zhang, M.Q.Li, Y.G.Liu, J.Luo, and T.Q.Liu, "The Growth Behavior of Austenite Grain in the Heating

Process of 300M Steel," *Materials Science and Engineering A*, vol. 528, pp. 4967-49-72, 2011.

[39] A.Roosz, Z.Cacsi, and E.G.Fuchs, "Iosthermal Formation of Austenite in Eutectoid Plain Carbon Steel," *Acta Metallurgica*, vol. 31, no. 4, pp. 509-517, 1983.

[40] D.V.Shtansky, K.Nakai, and Y.Ohmori, "Pearlite to Austenite Transformation in an Fe-2.6Cr-1C Alloy," *Acta Materialia*, vol. 47, no. 9, pp. 2619-2632, 1999.

[41] Sh.Matsuda and Y.Okamura, "Microstructural and Kinetic Studies of Reverse Transformation in a Low Carbon Low Alloy Steel," *Trans. Iron Steel Inst Jap*, vol. 14, no. 5, pp. 363-368, 1974.

[42] T.Shinozaki, Y.Tomota, T.Fukino, and T.Suzuki, "Microstructure Evolution during Reverse Transformation of Austenite from Tempered Martensite in Low Alloy Steel," *ISIJ International*, vol. 57, no. 3, p. 533–539, 2017.

[43] Zh.Jingwei, J.H.Lee, Y.W.Kim, Zh.Jiang, and Ch.S.Lee, "Enhancing Mechanical Properties of a Low-carbon Microalloyed Aast Steel by Controlled Heat Treatment," *Materials Science and Engineering A*, vol. 559, pp. 427-435, 2013.

[44] E.Abbasi and W.M.Rainforth, "Microstructural Evolution of Nb–V–Mo and V Containing TRIP-assisted Steels during Thermomechanical Processing," *Journal of Materials Science & Technology*, vol. 33, no. 4, pp. 311-320, 2017.

[45] Y.Tomota, W.Gong, S.Harjo, and T.Shinozaki, "Reverse Austenite Transformation Behavior in a Tempered Martensite Low-alloy Steel Studied Using in Situ Neutron Diffraction," *Scripta Materialia*, vol. 133, pp. 79-82, 2017.

[46] Sh.Matsuda and Y.OKamura, "The Later Stage of Reverse Transformation in Low Carbon Low Alloy Steel," *Trans. Iron Steel Inst. Jap*, vol. 14, no. 6, pp. 444-449, 1974.

[47] E.Abbasi and W.M.Rainforth, "Effect of Nb-Mo Additions on Precipitation Behaviour in V Microalloyed TRIP-assisted Steels," *Materials Science and Technology*, vol. 32, no. 16, pp. 1721-1729, 2016.

[48] L.Liu, Z.G.Yang, C.Zhang, and W.B.Liu, "An In Situ Study on Austenite Memory and Austenitic Spontaneous Recrystallization of a Martensitic Steel," *Materials Science and Engineering A*, vol. 527, pp. 7204-7209, 2010.

[49] E.I.Galindo-Nava and P.E.J.Rivera-Diaz-del-Castillo, "Understanding the Factors Controlling the Hardness in Martensitic Steels," *Scripta Materialia*, vol. 110, pp. 96-100, 2016.

[50] T.Furuhara, N.Takayama, and G.Miyamoto, "Key Factors in Grain Refinement of Martensite and Bainite," *Materials Science Forum*, vol. 638-642, pp. 3044-3049, 2010.

[51] Q.F.Guan, Q.C.Jiang, J.R.Fang, and H.Jiang, "Microstructures and Thermal Fatigue Behavior of Cr–Ni–Mo Hot Work Die Steel Modified by Rare Earth," *ISIJ International*, vol. 43, no. 5, p. 784–789, 2003.

[52] S.Morito, H.Yoshida, T.Makic, and X.Huang, "Effect of Block Size on the Strength of Lath Martensite in Low Carbon Steels," *Materials Science and Engineering A*, vol. 438–440, p. 237–240, 2006.

[53] F.Qian, J.Sharp, and W.M.Rainforth, "Microstructural Evolution of Mn-based Maraging Steels and Their Influences on Mechanical Properties," *Materials Science and Engineering A*, vol. 674, pp. 286-298, 2016.

[54] M.N.Shabrov, et al., "Void Nucleation by Inclusion Cracking," *Metallurgical and Materials Transactions*

*A*, vol. 35A, pp. 1745-1755, 2004.

[55] H.S.Yanga and H.K.D.H.Bhadeshia, "Austenite Grain Size and the Martensite-start Temperature," *Scripta Materialia*, vol. 60, p. 493–495, 2009.

[56] S.S.M.Tavares, J.M.Pardal, T.R.D.B.Martins, V.M.Schmitt, and J.F.V.Szlejf, "Influence of Austenitizing on the Mechanical Properties of Maraging 300 and Sae 4340 Steels – Comparative Study," *Materials Research*, pp. 1-8, 2017.

[57] R.O.Ritchie, B.Francis, and W.Server, "Evaluation of Toughness in AISI 4340 Alloy Steel Austenitized at Low and High Temperatures," *Metallurgical Transactions A*, vol. 7A, pp. 831-838, 1976.

[58] I.Tkalcec, D.Mari, and W.Benoit, "Correlation Between Internal Friction Background and the Concentration of Carbon in Solid Solution in a Martensitic Steel," *Materials Science and Engineering A*, vol. 442, pp. 471-475, 2006.

[59] S.Allain, O.Bouaziz, and M.Takahashi, "Toward a New Interpretation of the Mechanical Behaviour of As quenched Low Alloyed Martensitic Steels," *ISIJ International*, vol. 52, no. 4, pp. 717-722, 2012.

[60] Y.Lianga, et al., "The Important Role of Martensite Laths to Fracture Toughness for the Ductile Fracture Controlled by the Strain in EA4T Axle Steel," *Materials Science & Engineering A*, vol. 695, pp. 154-164, 2017.

[61] Y.Prawoto, N.Jasmawati, and K.Sumeru, "Effect of Prior Austenite Grain Size on the Morphology and Mechanical Properties of Martensite in Medium Carbon Steel," *Journal of Materials Science and Technology*, vol. 28, no. 5, pp. 464-466, 2012.

[62] S.Morito, H.Saito, T.Ogawa, T.Furuhara, and T.Maki, "Effect of Austenite Grain Size on the Morphology and Crystallorgaphy of Lath Martensite in Low Carbon Steels," *ISIJ International*, vol. 45, no. 1, pp. 91-94, 2005.

[63] C.Du, J.P.M.Hoefnagels, R.Vaes, and M.G.D.Geers, "Block and Sub-block Boundary Strengthening in Lath Martensite," *Scripta Materialia*, vol. 116, pp. 117-121, 2016.

[64] A.Salemi and A.Abdollah-zadeh, "The Effect of Tempering Temperature on the Mechanical Properties and Fracture Morphology of a NiCrMoV Steel," *Materials Characterization*, vol. 59, p. 484–487, 2008.

[65] T.Xu, Zh.Jin, Y.Feng, Sh.Song, and D.Wang, "Study on the Static and Dynamic Fracture Mechanism of Different Casing Drilling Steel Grades," *Materials Characterisation*, vol. 67, pp. 1-9, 2012.

[66] E.A.Little, D.R.Harries, F.B.Pickering, and S.R.Keown, "Effects of Heat Treatment on Structure and Properties of 12%Cr Steels," *Metals Technology*, vol. 4, no. 1, pp. 205-217, 1977.

[67] Sh.l.Long, et al., "Effect of Quenching Temperature on Martensite Multi-level Microstructures and Properties of Strength and Toughness in 20CrNi2Mo Steel," *Materials Science and Engineering A*, vol. 676, pp. 38-47, 2016.